Cell

Glycosylation-Dependent Lectin-Receptor Interactions Preserve Angiogenesis in Anti-VEGF Refractory Tumors

Diego O. Croci,[1] Juan P. Cerliani,[1] Tomas Dalotto-Moreno,[1] Santiago P. Méndez-Huergo,[1] Ivan D. Mascanfroni,[1] Sebastián Dergan-Dylon,[1] Marta A. Toscano,[1] Julio J. Caramelo,[2] Juan J. García-Vallejo,[3] Jing Ouyang,[4] Enrique A. Mesri,[5] Melissa R. Junttila,[6] Carlos Bais,[6] Margaret A. Shipp,[4] Mariana Salatino,[1] and Gabriel A. Rabinovich[1,7,*]

[1]Laboratorio de Inmunopatología, Instituto de Biología y Medicina Experimental (IBYME), Consejo Nacional de Investigaciones Científicas y Técnicas (CONICET), 1428 Buenos Aires, Argentina

[2]Laboratorio de Biología Estructural y Celular, Fundación Instituto Leloir, CONICET, 1405 Buenos Aires, Argentina

[3]Department of Molecular Cell Biology and Immunology, VU University Medical Center, 1081BT Amsterdam, The Netherlands

[4]Department of Medical Oncology, Dana Farber Cancer Institute, Boston, MA 02215, USA

[5]Miami Center for AIDS Research, Department of Microbiology and Immunology, Sylvester Comprehensive Cancer Center, University of Miami Miller School of Medicine, Miami, FL 33136, USA

[6]Genentech, Inc., South San Francisco, CA 94080, USA

[7]Laboratorio de Glicómica. Departamento de Química Biológica, Facultad de Ciencias Exactas y Naturales, Universidad de Buenos Aires, 1428 Buenos Aires, Argentina

*Correspondence: gabyrabi@gmail.com

http://dx.doi.org/10.1016/j.cell.2014.01.043

SUMMARY

The clinical benefit conferred by vascular endothelial growth factors (VEGF)-targeted therapies is variable, and tumors from treated patients eventually reinitiate growth. Here, we identify a glycosylation-dependent pathway that compensates for the absence of cognate ligand and preserves angiogenesis in response to VEGF blockade. Remodeling of the endothelial cell (EC) surface glycome selectively regulated binding of galectin-1 (Gal1), which upon recognition of complex *N*-glycans on VEGFR2, activated VEGF-like signaling. Vessels within anti-VEGF-sensitive tumors exhibited high levels of α2-6-linked sialic acid, which prevented Gal1 binding. In contrast, anti-VEGF refractory tumors secreted increased Gal1 and their associated vasculature displayed glycosylation patterns that facilitated Gal1-EC interactions. Interruption of β1-6GlcNAc branching in ECs or silencing of tumor-derived Gal1 converted refractory into anti-VEGF-sensitive tumors, whereas elimination of α2-6-linked sialic acid conferred resistance to anti-VEGF. Disruption of the Gal1-*N*-glycan axis promoted vascular remodeling, immune cell influx and tumor growth inhibition. Thus, targeting glycosylation-dependent lectin-receptor interactions may increase the efficacy of anti-VEGF treatment.

INTRODUCTION

Genetic and pharmacological disruption of vascular signaling pathways have provided unequivocal evidence that abnormal angiogenesis is a hallmark feature of cancer (Chung and Ferrara, 2011; Potente et al., 2011). Vascular endothelial growth factors (VEGFs) play central roles in this process through activation of VEGF receptor tyrosine kinases (RTKs), including VEGFR1 (Flt-1), VEGFR2 (KDR/Flk-1), and VEGFR3 (Flt-4) on endothelial cells (ECs) (Chung and Ferrara, 2011). Blockade of VEGF-A signaling with bevacizumab, a humanized anti-VEGF monoclonal antibody (mAb), or with RTK inhibitors has improved progression-free survival and, in some indications overall survival, across several types of cancers, including metastatic colorectal cancer, non-small-cell lung cancer, metastatic breast cancer, renal cell carcinoma, and hepatocarcinoma (Ellis and Hicklin, 2008). However, the clinical benefit conferred by these therapies is variable, and tumors from treated patients eventually reinitiate growth (Ebos et al., 2009).

It has been suggested that induction of compensatory angiogenic pathways may contribute to limit the efficacy of anti-VEGF treatment. This proposition is supported by preclinical data showing the release of alternative proangiogenic signals and the mobilization of angio-competent bone marrow-derived myeloid cells by anti-VEGF refractory tumors (Bergers and Hanahan, 2008). Future antiangiogenic therapies should capitalize on an improved understanding of these compensatory pathways as well as the identification of hallmark signatures that can delineate sensitivity to anti-VEGF treatment.

Programmed remodeling of cell-surface glycans through the sequential action of glycosyltransferases and glycosidases regulates a variety of physiologic and pathologic processes (Ohtsubo and Marth, 2006; Hart and Copeland, 2010). Glycosylation controls EC biology by modulating Notch receptor signaling (Benedito et al., 2009), sustaining EC survival (Kitazume et al., 2010), regulating vascular permeability (Xu et al., 2011), and connecting blood and lymphatic vessels (Fu et al., 2008). Likewise, changes in the cellular glycome could alter vascular processes by displaying or masking ligands for endogenous lectins, which

translate glycan-containing information into functional cellular responses (Rabinovich and Croci, 2012). Galectin-1 (Gal1), a member of a conserved family of animal lectins, promotes tumor progression through mechanisms leading to tumor-immune escape and metastasis (Rubinstein et al., 2004; Banh et al., 2011; Dalotto-Moreno et al., 2013). Interestingly, Gal1 is regulated by hypoxia (Le et al., 2005; Croci et al., 2012) and controls EC signaling (Hsieh et al., 2008), VEGFR trafficking (D'Haene et al., 2013), and tumor angiogenesis (Thijssen et al., 2006, 2010; Mathieu et al., 2012; Laderach et al., 2013). Here, we evaluated the hypothesis that Gal1 association with glycosylated EC receptors might link tumor hypoxia to angiogenic compensatory programs in response to VEGF blockade.

RESULTS

Context-Dependent Regulation of the EC Glycome Controls Gal1 Binding and Angiogenesis

We first examined the "glycosylation signature" of human ECs at baseline and following exposure to physiologically relevant stimuli. We used a panel of lectins that recognize specific glycan structures, including those that are relevant for Gal1 binding. Gal1 recognizes multiple galactose-β1-4-*N*-acetylglucosamine (LacNAc) units, which are present on the branches of *N*- or *O*-linked glycans and are created by the concerted action of specific glycosyltransferases. This includes the *N*-acetylglucosaminyltransferase 5 (MGAT5), an enzyme that generates β1-6-*N*-acetylglucosamine (β1-6GlcNAc)-branched complex *N*-glycans, which are the preferred intermediates for LacNAc extension (Figure 1A). Under resting conditions, primary human umbilical vein ECs (HUVEC) showed considerable expression of L-phytohemagglutinin (L-PHA)-reactive MGAT5-modified *N*-glycans and *Lycopersicon esculentum* lectin (LEL)-reactive poly-LacNAc ligands, which increased significantly following exposure to immunosuppressive cytokines (IL-10 or TGF-β_1) or to proangiogenic FGF2 (Figures 1B and 1C). In contrast, ECs exposed to proinflammatory T_H1 (IFN-γ) or T_H17 (IL-17) cytokines showed significantly lower L-PHA reactivity (Figure 1C). As α2-6 sialyltransferase (ST6GAL1) may modify LacNAc ligands and block Gal1 signaling (Toscano et al., 2007), we then examined binding of *Sambucus nigra* agglutinin (SNA), a lectin that recognizes α2-6-linked sialic acid (SA). Stimulation of ECs with FGF2 or a combination of IL-10 and TGF-β_1 led to reduction of SNA-reactive glyco-epitopes, as compared to resting, IL-17- or IFN-γ-treated ECs (Figures 1B and 1C), suggesting that pro- or anti-inflammatory signals may either mask or unmask Gal1-specific binding sites. In contrast, ECs showed similar binding profiles for the *Maackia amurensis* agglutinin (MAL II), which recognizes α2-3 SA linkages, regardless of the stimulus used (Figures 1B and 1C).

Exposure of Gal1-specific glyco-epitopes may also be regulated by the core-2 β1-6-*N*-acetylglucosaminyltransferase 1 (C2GNT1), which acts on asialo-galactose-β1-3-*N*-acetylgalactosamine core 1 *O*-glycans to synthesize the core 2 branching structure (Figure 1A). Exposure of HUVEC to FGF2, IL-10, or TGF-β_1 resulted in modest increase of peanut agglutinin (PNA)-reactive asialo-core-1 *O*-glycans, compared to cells exposed to IFN-γ or IL-17 (Figures 1B and 1C). However, we observed no significant binding of the α-N-acetyl-galactosamine-reactive *Helix pomatia* agglutinin (HPA) (Figure 1B). Moreover, exposure to VEGF-A resulted in no significant changes in the EC glycophenotype (Figure 1C). Thus, immunosuppressive stimuli favor a Gal1-permissive glycophenotype on ECs, while proinflammatory signals reduce expression of these glyco-epitopes. Similar results were observed using the mouse EC line EOMA (data not shown).

To determine the contribution of EC surface glycosylation to Gal1 function, we examined Gal1 binding to ECs under different experimental conditions. Gal1 bound to ECs in a dose- and carbohydrate-dependent fashion (Figure 1D). Accordingly, a Gal1 mutant lacking carbohydrate-binding activity ($Gal1^{N46D}$) did not bind to ECs at any of the concentrations tested (Figure 1D). While Gal1 binding was almost completely abrogated by swainsonine, an inhibitor of *N*-glycan biosynthesis, benzyl-α-GalNAc, an inhibitor of *O*-glycan elongation, was only partially inhibitory (Figure 1D), suggesting the essential contribution of *N*-glycans to Gal1 signaling. Moreover, decrease of *N*-glycan branching through siRNA-mediated silencing of MGAT5 almost completely eliminated Gal1 binding, whereas inhibition of core 2 *O*-glycan elongation through C2GNT1 silencing had no effect (Figure 1E and Figures S1A, and S1B available online). Consistent with changes in glycosylation, Gal1 binding was higher in ECs exposed to immunosuppressive stimuli compared to cells sensing proinflammatory cytokines (Figure 1F).

Because hypoxia fuels activation of angiogenic rescue programs (Potente et al., 2011), we asked whether hypoxic microenvironments could influence the EC glycan profile. Hypoxia increased the amounts of β1-6GlcNAc-branched *N*-glycans and poly-LacNAc structures, reduced α2-6 sialylation, and induced slight changes in asialo-core-1 *O*-glycans in comparison to normoxia (Figure 1G). These results were substantiated by glycan nanoprofiling, which documented an increase in the relative abundance of neutral *N*-glycans and a decrease in tri- and tetra-sialylated *N*-glycans on ECs exposed to hypoxia (Figures 1H and S1C). Accordingly, we found higher binding of Gal1 to ECs cultured under hypoxic conditions (Figure 1I).

We then analyzed the contribution of *N*- and *O*-glycans to the proangiogenic functions displayed by Gal1 and VEGF-A. Addition of lactose or decrease of *N*-glycan branching through MGAT5 silencing or swainsonine treatment almost completely prevented EC proliferation, migration, and tube formation induced by Gal1, while silencing C2GNT1 had no effect. Accordingly, exposure to $Gal1^{N46D}$ mutant had no impact on EC responses (Figures 1J and S1D–S1F). In contrast, the proangiogenic effects of VEGF-A were preserved regardless of the absence or presence of complex *N*- or *O*-glycan branching (Figures 1J and S1D–S1E). Thus, unlike VEGF-A, Gal1 delivers proangiogenic signals through a glycosylation-dependent pathway involving context-dependent remodeling of complex *N*-glycans.

Glycosylation-Dependent Binding of Gal1 to ECs Mimics VEGF-A Function

To integrate the Gal1-*N*-glycan axis into canonical angiogenic circuits, we studied the molecular basis of Gal1-receptor interactions. Screening for changes in the phosphorylation status of a spectrum of growth factor RTKs and signaling nodes revealed

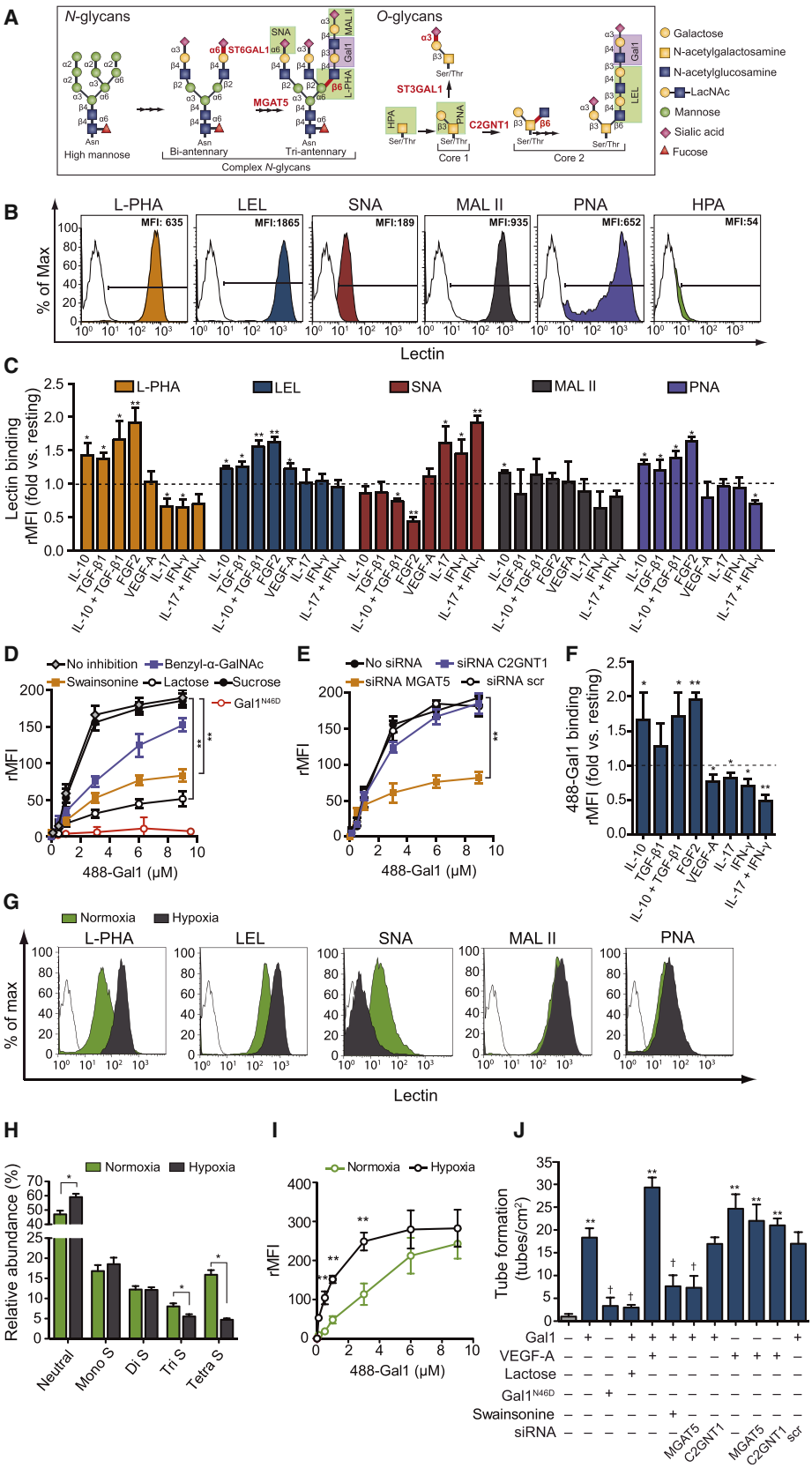

(legend on next page)

that VEGFR2 was the only tested RTK that became phosphorylated following treatment of ECs with Gal1 (Figures 2A and S2A). This phosphorylation pattern was detected at 15 min (Figure 2A) and was sustained after 60 min of exposure to this lectin (data not shown). In addition, Gal1 increased the phosphorylation of Akt (Thr^{308}), Akt (Ser^{473}), and Erk1/2, recapitulating the phosphorylation pattern elicited by VEGF-A (Figures 2A, S2B, and S2C). Silencing VEGFR2 almost completely prevented Akt and Erk1/2 phosphorylation induced by either Gal1 or VEGF-A (Figure 2B and S2D) and abrogated Gal1-induced EC migration and tube formation (Figures 2C, 2D, S2E, and S2F). In contrast, blockade of VEGFR1, VEGFR3, or integrins $\alpha_v\beta_3$ or $\alpha_5\beta_1$ had no effect on Gal1-induced EC functions (Figure 2D). Likewise, silencing neuropilin-1 (NRP-1), a recognized Gal1-binding partner (Hsieh et al., 2008), had no significant impact on Gal1 function (Figure 2C, S2D, and S2E). Because of the autocrine effects of VEGF signaling (Lee et al., 2007), we examined whether Gal1 signaling proceeded in the absence of VEGF-A. Consistent with lack of effect of Gal1 on VEGF-A secretion (Figure S2G), inhibition of intracellular or extracellular VEGF-A had no influence on Gal1 effects (Figures 2C, 2D, S2E, S2F, and S2H). Similarly, FGF2 blockade did not alter Gal1 activity (Figure S2F).

As branching of complex *N*-glycans may fine-tune the threshold for growth factor signaling (Dennis et al., 2009; Song et al., 2010), we further investigated whether MGAT5-modified glycans can modulate sensitivity of VEGFR2 to its canonical ligand VEGF-A. Targeting MGAT5 selectively eliminated responsiveness to Gal1, but it had no impact on VEGF signaling (Figure 2B). In contrast, blockade of core 2 *O*-glycan elongation had no effect on Gal1 or VEGF-A signaling (data not shown). Hence, rather than altering VEGF-A signaling, Gal1 directly co-opts the VEGFR2 pathway through binding to complex *N*-glycans. Coimmunoprecipitation experiments with HUVEC treated with Gal1 in the absence or presence of PNGase F or following transfection with MGAT5 or C2GNT1 siRNA revealed that Gal1 associated with VEGFR2 through *N*-glycosylation-dependent mechanisms (Figure 2E). These interactions were confirmed by Föster resonance energy transfer (FRET) analysis of 594-Gal1 binding to fully-glycosylated 488-VEGFR2, which revealed a bimodal behavior and a dissociation constant (K_d) within the low micromolar range (Figures 2F and S2I). Titration of the Gal1-VEGFR2 complex with lactose confirmed the glycan dependence of these interactions showing a considerable increase of 488-VEGFR2 fluorescence, which displayed a hyperbolic behavior and revealed an apparent K_d of 250 μM (Figure 2F), similar to that calculated for the Gal1-lactose complex (López-Lucendo et al., 2004). Immunoprecipitation followed by lectin blotting revealed considerably lower amounts of α2-6-linked SA in VEGFR2 compared to VEGFR1, consistent with the preferential association of Gal1 with VEGFR2 (Figure 2G).

VEGFR2 is organized into seven extracellular immunoglobulin (Ig)-like folds and contains 18 putative *N*-linked glycosylation sites. While Ig-2 and -3 mediate VEGF-A binding, Ig-4 to -6 control receptor dimerization and Ig-7 stabilizes dimer formation (Olsson et al., 2006). To identify which domains are responsible for Gal1 binding, we prepared a series of human VEGFR2 mutants that are devoid of *N*-glycosylation sites in each of the seven Ig-like domains (Figure S2J). The HA-tagged wild-type (WT) and VEGFR2 mutants were stably expressed in HEK293T cells, showing comparable total and cell-surface expression (Figure S2K). Using anti-HA-conjugated 633-fluorescent beads, we immunoprecipitated VEGFR2 variants and examined binding of 488-Gal1 to immunoprecipitates. Flow cytometry of double-positive beads revealed that mutations in *N*-glycosylation sites of Ig-3 (N245Q, N318Q), Ig-4 (N374Q, N395Q), and Ig-7 (N675Q, N704Q, N721Q) partially prevented Gal1 binding (Figure 2H), suggesting major contributions of these domains to glycan-dependent recognition of this lectin. Binding of Gal1 resulted in *N*-glycan-dependent segregation of VEGFR2 to membrane patches, indicating rearrangement of signaling clusters on the EC surface (Figure 2I). Moreover, this lectin-modulated cell-surface residency of VEGFR2 and its internalization, which occurred with slower kinetics than those triggered by VEGF-A (Figures 2J, S2L, and S2M). Thus, Gal1 co-opts the VEGFR2 signaling pathway through binding to nonsialylated *N*-glycans on this RTK.

Differential Glycosylation of Tumor-Associated Vasculature Delineates Sensitivity to Anti-VEGF Treatment

To investigate whether the Gal1-*N*-glycan axis preserves vascularization in anti-VEGF refractory tumors, we evaluated changes in the "glycosylation signature" of ECs associated with tumors that are known to be sensitive (B16-F0 melanoma and CT26 colon carcinoma) or refractory (LLC1 Lewis lung

Figure 1. Remodeling of the EC Glycome Controls Gal1 Function

(A) Schematic representation of *N*- and *O*-glycan biosynthesis.

(B) Glycophenotype of resting HUVEC detected with biotinylated lectins (filled) or with PE-conjugated streptavidin alone (open). Representative of eight experiments.

(C) Glycophenotype of HUVEC treated with different stimuli (rMFI [relative mean fluorescence intensity] = (MFI with lectin – MFI without lectin)/MFI without lectin). Presented as ratio relative to resting conditions (dotted line) (mean ± SEM, n = 4; *p < 0.05, **p < 0.01 versus resting).

(D and E) Binding of 488-Gal1 or 488-$Gal1^{N46D}$ to HUVEC treated with inhibitors (D) or transfected with specific siRNA (E) (mean ± SEM, n = 4; **p < 0.01).

(F) Binding of 488-Gal1 to HUVEC treated with different stimuli (mean ± SEM, n = 4; *p < 0.05, **p < 0.01 versus resting).

(G) Glycophenotype of HUVEC cultured in hypoxia (gray) or normoxia (green) detected with biotinylated lectins or with PE-conjugated streptavidin alone (open). Representative of five experiments.

(H) Glycan nanoprofiling of HUVEC exposed to normoxia or hypoxia (mean ± SEM, n = 3; *p < 0.05).

(I) Binding of 488-Gal1 to HUVEC exposed to hypoxia or normoxia (mean ± SEM, n = 5; **p < 0.01).

(J) Tube formation of HUVEC transfected or not with specific siRNA and incubated with Gal1 (1 μM), $Gal1^{N46D}$ (3 μM) and/or VEGF-A (20 ng/ml) with or without inhibitors (mean ± SEM, n = 5, **p < 0.01 versus control, †p < 0.05 versus Gal1).

See also Figure S1.

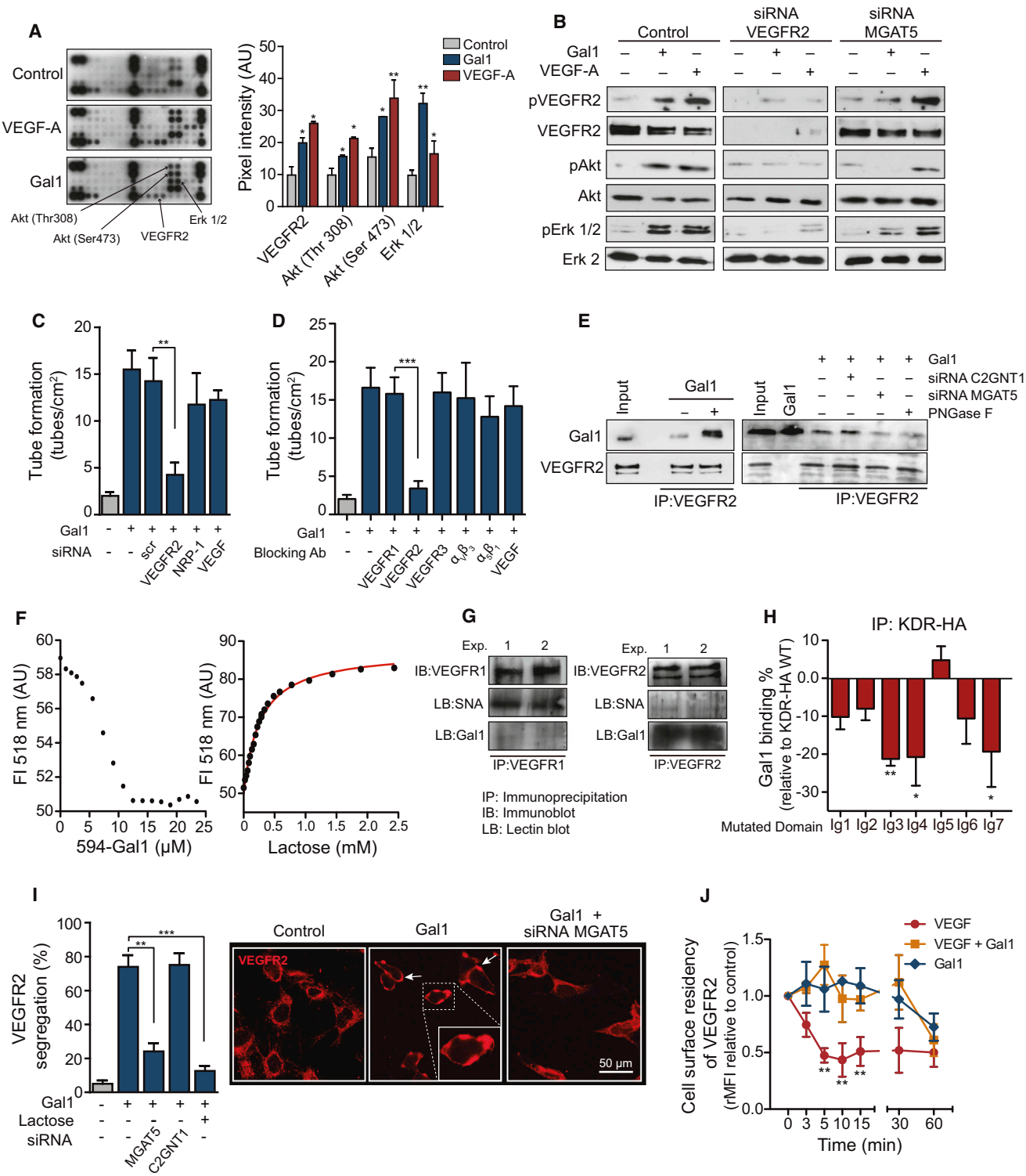

Figure 2. Glycosylation-Dependent Binding of Gal1 to ECs Mimics VEGF-A Function

(A) Phospho-RTK signaling array of HUVEC exposed to medium, VEGF-A, or Gal1. Right: quantification of pixel intensity (mean ± SEM, n = 4; *p < 0.05, **p < 0.01 versus control).

(B) Immunoblot of phosphorylated and total VEGFR2, Akt and Erk1/2 in HUVEC transfected or not with specific siRNA and treated with Gal1 (1 μM) or VEGF-A (20 ng/ml). Representative of three experiments.

(legend continued on next page)

carcinoma and R1.1 T cell lymphoma) to anti-VEGF treatment (Shojaei et al., 2007). We confirmed marked inhibition of tumor growth and reduced vascular supply in B16-F0- and CT26-sensitive tumors implanted into syngeneic mice and treated with the anti-VEGF mAb, whereas growth and vascularization of LLC1 and R1.1 refractory tumors were only transiently and poorly inhibited (Figures 3A and 3B). In vitro, conditioned media (CM) from LLC1 and R1.1 cells that were previously exposed to hypoxia induced consistent changes in the glycan repertoire of ECs, as reflected by diminished display of α2-6-linked SA, greater exposure of β1-6-branched *N*-glycans and increased frequency of poly-LacNAc-extended glycans, compared to ECs exposed to CM from tumor cells cultured in normoxia (Figure 3C). Accordingly, we found higher binding of Gal1 to ECs exposed to CM from LLC1 tumor cells cultured in hypoxic conditions (Figure S3A). Induction of a "Gal1-permisive" glycan repertoire was a feature of anti-VEGF refractory but not sensitive tumors, as B16-F0 and CT26 cells were unable to promote changes in the EC glycophenotype when exposed to hypoxia (Figure 3C). This differential responses could not be attributed to selective upregulation of proangiogenic factors (FGF2, TGF-β_1, or VEGF-A) by different tumor cell lines (Figure S3B). Thus, hypoxia acts as a major driving force that instructs anti-VEGF refractory but not sensitive tumors to selectively alter the EC glycan profile.

To evaluate changes in the glycophenotype of tumor-associated vessels in vivo, mice were implanted with sensitive or refractory tumors and treated with anti-VEGF or control mAb when tumors reached 100 mm^3. Four and 7 days after anti-VEGF treatment, vessels within refractory tumors showed reduced α2-6 sialylation and higher β1-6 *N*-glycan branching (Figure 3D). Refractoriness was also associated with higher secretion of Gal1, but not other proangiogenic galectins by tumor cells (Figures 3F and S3C). In contrast, vessels within sensitive tumors showed no significant alterations of the EC glycophenotype and no changes in Gal1 secretion in response to VEGF blockade (Figures 3E and 3F). Thus, anti-VEGF refractory tumors selectively respond to VEGF blockade by upregulating Gal1 expression and modulating the EC-associated glycan profile. Based on these findings, we sought to analyze Gal1 expression in tumors obtained from a *Kras*-driven genetically engineered mouse model of pancreatic ductal adenocarcinoma (PDAC), which responds to anti-VEGF treatment with no changes in progression-free or overall survival (Singh et al., 2010). We found higher Gal1 expression in anti-VEGF-treated versus anti-ragweed-treated PDAC tumors (Figure S3D), thus substantiating the robust upregulation of this lectin in tumors with limited responses to anti-VEGF treatment.

Tumor Depletion of Gal1 Confers Sensitivity to Anti-VEGF Treatment

To explore the relative contribution of Gal1 to anti-VEGF sensitivity, syngeneic mice were implanted with LLC1 or R1.1 tumors expressing shRNA-Gal1 constructs and treated with anti-VEGF mAb when tumors reached 100 mm^3. Silencing Gal1 increased sensitivity to anti-VEGF treatment in both LLC1 and R1.1 tumors, as evidenced by diminished tumor burden (Figures 4A and S4A) and vascularization (Figure 4B) following injection of anti-VEGF mAb. This effect was not due to differences in in vitro proliferation between WT and knockdown tumors (Figure S4B). Tumor growth inhibition was not further enhanced when Gal1 knockdown LLC1 cells were inoculated into syngeneic Gal1-deficient (*Lgals1*$^{-/-}$) mice (Figure 4C), suggesting no substantial contribution of host-derived Gal1 to this effect. On the other hand, targeting Gal1 in anti-VEGF-sensitive B16-F0 tumors induced only a slight improvement of the therapeutic benefits of VEGF blockade (Figures 4D, 4E, and S4C). These changes were not associated with undesired off-target effects as Gal1, but not other relevant tumor galectins, was altered following Gal1 shRNA transduction (Figures S4A and S4D). Thus, targeting Gal1 in the tumor microenvironment may help to increase the efficacy of anti-VEGF treatment.

Reprogramming of EC Glycosylation Modulates Tumor Sensitivity to Anti-VEGF

To investigate the relevance of EC glycosylation in anti-VEGF compensatory programs, we implanted anti-VEGF refractory or sensitive tumors into glycosyltransferase-deficient mice. Given the selective upregulation of β1-6GlcNAc-branched *N*-glycans in vessels associated with anti-VEGF refractory tumors (Figure 3D), we sought to elucidate the contribution of this pathway to the compensatory angiogenic phenotype. Mice lacking MGAT5 were implanted with the LLC1 refractory tumor and treated with anti-VEGF or control mAb. Lack of PHA reactivity confirmed the absence of β1-6GlcNAc-branched oligosaccharides in tumor-associated ECs from *Mgat5*$^{-/-}$ mice (Figure 5A). Anti-VEGF treatment in *Mgat5*$^{-/-}$ mice led to marked inhibition of tumor growth and vascularization compared to their WT counterparts (Figures

(C and D) Tube formation of HUVEC transfected or not with specific siRNA (C) or incubated with relevant blocking Ab (D) and treated or not with Gal1 (mean ± SEM, n = 4; **p < 0.01; ***p < 0.001).

(E) Coimmunoprecipitation followed by immunoblot of Gal1 and VEGFR2 of HUVEC treated with or without Gal1 (left) or treated with Gal1 following transfection with specific siRNA or treatment with PNGase F. Input, whole-cell lysate. Representative of three experiments.

(F) Binding of 594-Gal1 to 488-rhVEGFR2 followed by FRET. Left: fluorescence intensity (518 nm). Right: fluorescence intensity of 0.5 μM 488-VEGFR2 in the presence of 594-Gal1 titrated with lactose. Representative of three experiments.

(G) Immunoprecipitaton of VEGFR1 and VEGFR2 followed by lectin blotting. Two representative of three experiments are shown.

(H) Binding of Gal1 to immunoprecipitated KDR-HA mutants lacking *N*-glycosylation sites in Ig-like domains (mean ± SEM, n = 4; *p < 0.05, **p < 0.01 versus WT-KDR).

(I) Confocal microscopy of VEGFR2 segregation in HUVEC transfected or not with specific siRNA and treated with Gal1 or Gal1 plus lactose (mean ± SEM [left] or representative [right], n = 4; **p < 0.01, ***p < 0.001).

(J) Flow cytometry of VEGFR2 in nonpermeabilized HUVEC treated with VEGF-A, Gal1 or VEGF-A plus Gal1 (mean ± SEM, n = 4; **p < 0.01).

See also Figure S2.

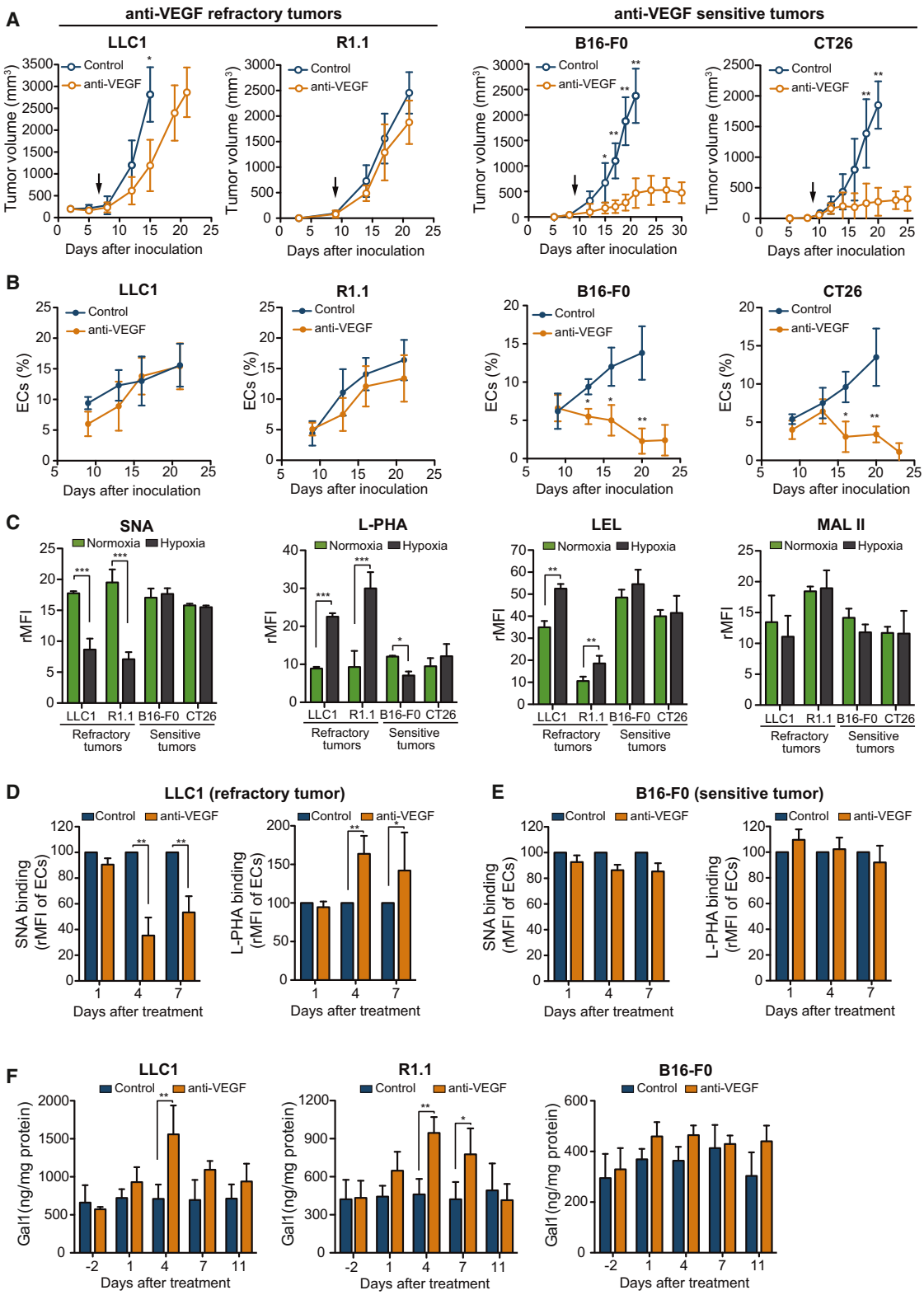

Figure 3. Differential Glycosylation of Tumor-Associated Vasculature Delineates Sensitivity to Anti-VEGF Treatment

(A and B) Tumor growth (A) and percentage of tumor-associated ECs (B) in mice inoculated with the indicated tumors and treated with anti-VEGF (5 mg/kg) or control mAb (mean ± SEM, n = 4, six animals per group; *p < 0.05, **p < 0.01).

(legend continued on next page)

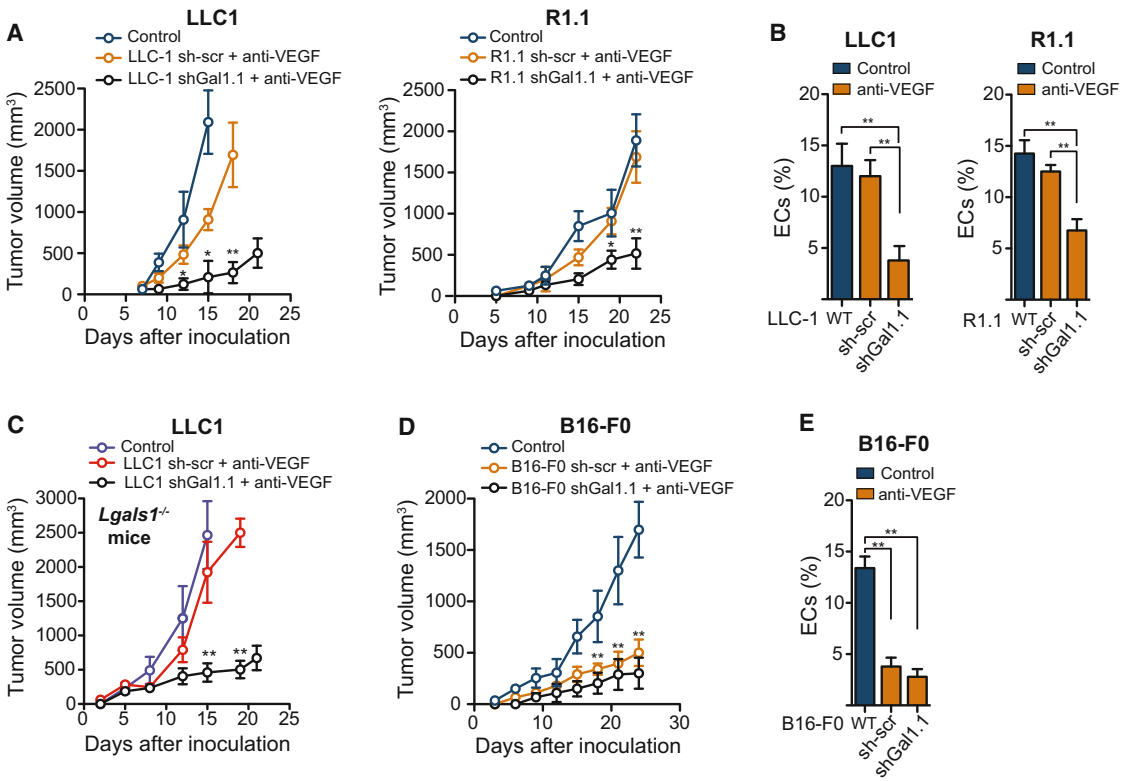

Figure 4. Tumor Depletion of Gal1 Confers Sensitivity to Anti-VEGF Treatment

(A and B) Tumor growth (A) and percentage of tumor-associated ECs (B) in B6 mice inoculated with LLC1 or R1.1 tumors transduced with Gal1-specific shRNA (shGal1.1) or sh-scr and treated with anti-VEGF or control mAb (mean ± SEM, n = 4 with six animals per group; *p < 0.05; **p < 0.01).

(C) Tumor growth in *Lgals1*$^{-/-}$ B6 mice inoculated with LLC1 tumors transduced with shGal1.1 or sh-scr and treated with anti-VEGF or control mAb (mean ± SEM, n = 3 with six animals per group; **p < 0.01).

(D, E) Tumor growth (D) and percentage of tumor-associated ECs (E) in B6 mice inoculated with B16-F0 tumors transduced with shGal1.1 or sh-scr and treated with anti-VEGF or control mAb (mean ± SEM, n = 4 with six animals per group; **p < 0.01).

See also Figure S4.

5B and 5C). Thus, lack of β1-6GlcNAc-branched *N*-glycans in tumor-associated vessels converted otherwise refractory into anti-VEGF-sensitive tumors.

Because α2-6-linked SA is highly represented in the vasculature of anti-VEGF-sensitive tumors, we hypothesized that lack of α2-6 sialylation may render tumors insensitive to anti-VEGF treatment. Mice lacking ST6GAL1 were implanted with the B16-F0-sensitive tumor and treated with anti-VEGF or control mAb. Lack of SNA reactivity confirmed the absence of α2-6-linked SA in tumor-associated vessels (Figure 5D). Loss of α2-6-sialylation in tumor-associated vasculature conferred reduced sensitivity to anti-VEGF treatment, as shown by increased tumor growth and formation of a highly dense tumor vascular network (Figures 5E and 5F). This phenotype could be rescued when *St6gal1*$^{-/-}$ mice were challenged with Gal1-deficient B16 tumors and further treated with anti-VEGF mAb (Figure 5G), suggesting that loss of α2-6-linked SA may enhance vascular signaling by unmasking Gal1-specific ligands. Furthermore, this compensatory program was suppressed when *St6gal1*$^{-/-}$ mice were implanted with B16 tumors and further treated with anti-VEGF mAb in the presence of the RTK inhibitor axitinib, which preferentially suppresses VEGFRs signaling (Figure 5G). However, no changes in tumor growth or vascularization were observed in response to VEGF blockade when a sensitive tumor was inoculated into *Mgat5*$^{-/-}$ mice or when a refractory tumor was grown in *St6gal1*$^{-/-}$ mice (data not shown). Thus, reprogramming of the EC glycome, leading to disruption of Gal1-specific ligands, may contribute to circumvent refractoriness to anti-VEGF treatment.

(C) Glycophenotype of ECs exposed to serum-free conditioned media from the indicated tumor cells previously cultured in normoxia or hypoxia (mean ± SEM, n = 4; *p < 0.05, **p < 0.01, ***p < 0.001).

(D and E) Glycophenotype of vessels associated to LLC1 (D) or B16-F0 (E) tumors in response to anti-VEGF treatment in vivo (mean ± SEM, n = 4; six animals per group *p < 0.05, **p < 0.01).

(F) ELISA of Gal1 secretion by different tumors in response to anti-VEGF treatment (mean ± SEM, n = 4; *p < 0.05, **p < 0.01).

See also Figure S3.

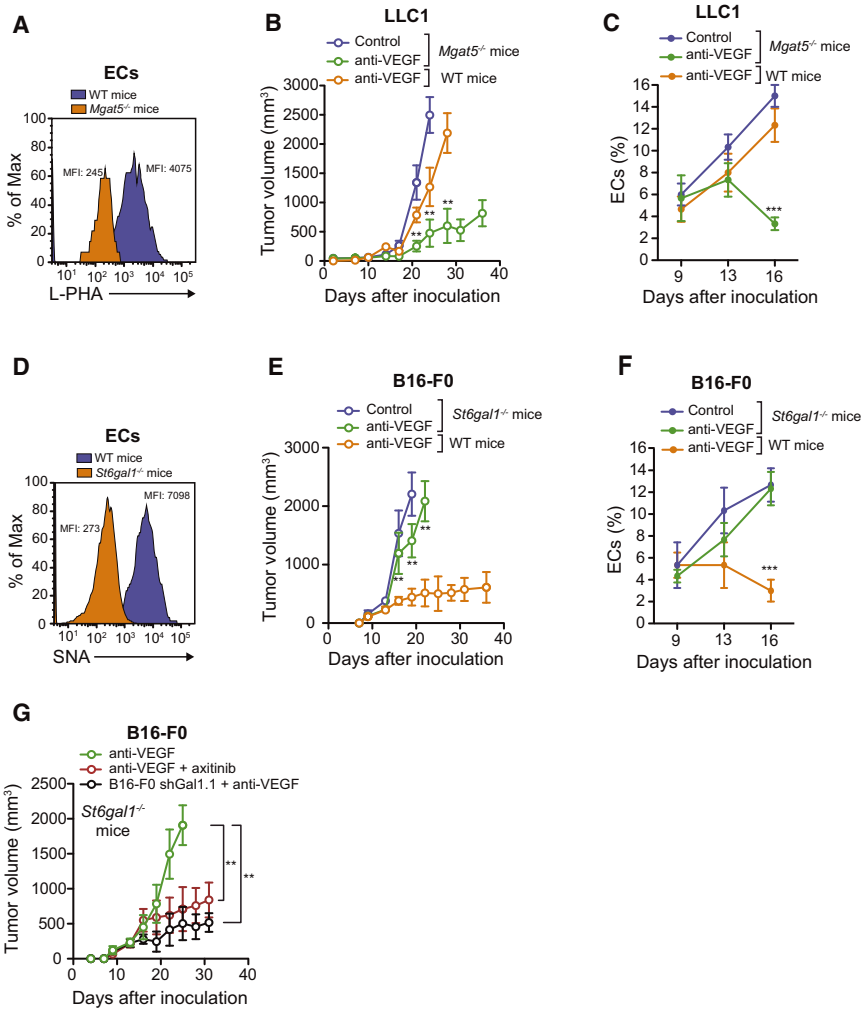

Figure 5. Reprogramming of EC Glycosylation Modulates Tumor Sensitivity to Anti-VEGF

(A) Flow cytometry of L-PHA binding to ECs associated to LLC1 tumors inoculated into WT or *Mgat5*$^{-/-}$ mice (day 16). Representative of four experiments with six animals per group.

(B and C) Tumor growth (B) and percentage of tumor-associated ECs (C) in *Mgat5*$^{-/-}$ or WT mice inoculated with LLC1 tumors and treated with anti-VEGF or control mAb (5 mg/kg) (mean ± SEM, n = 4 with six animals per group; **p < 0.01, ***p < 0.001).

(D) Flow cytometry of SNA binding to ECs associated to B16-F0 tumors inoculated into WT or *St6gal1*$^{-/-}$ mice (day 16). Representative of four experiments with six animals per group.

(E and F) Tumor growth (E) and percentage of tumor-associated ECs (F) in *St6gal1*$^{-/-}$ or WT mice inoculated with B16-F0 tumors and treated with anti-VEGF or control mAb (mean ± SEM, n = 4 with six animals per group; **p < 0.01, ***p < 0.001).

(G) Tumor growth in *St6gal1*$^{-/-}$ mice inoculated with B16-F0 tumors and treated with anti-VEGF mAb or with anti-VEGF mAb plus axitinib (30 mg/kg) or inoculated with B16-F0 tumors transduced with Gal1-specific shRNA (shGal1.1) and treated with anti-VEGF mAb (mean ± SEM, n = 3 with six animals per group; **p < 0.01).

Targeting the Gal1-*N*-Glycan Axis Overcomes Refractoriness to Anti-VEGF Treatment and Promotes Vascular Remodeling

In the quest for a therapeutic agent capable of defeating anti-VEGF refractoriness, we evaluated the therapeutic effects of a function-blocking Gal1 mAb (F8.G7) selected by its ability to neutralize Gal1, but not other galectins (Croci et al., 2012). This mAb specifically prevented tube formation and EC migration induced by Gal1, but not VEGF-A (Figures 6A and S5A), and inhibited Gal1-induced VEGFR2 phosphorylation to levels comparable to those attained by MGAT5 silencing (Figure 6B).

Administration of F8.G7 mAb (10 mg/kg) successfully circumvented anti-VEGF refractoriness displayed by LLC1 and R1.1 tumors, as evidenced by reduced tumor growth and vascularization at day 7 following combined treatment (Figures 6C and 6D). On the other hand, Ab-mediated Gal1 blockade slightly enhanced the therapeutic benefit of anti-VEGF in the sensitive B16 tumors (Figure 6E). Remarkably, single administration of F8.G7 mAb afforded sustained inhibition of tumor growth and vascularization in mice bearing refractory or sensitive tumors (Figures 6C–6E and S5B). Of note, the amounts of secreted Gal1 varied considerably among different inoculated tumor types but dropped substantially following administration of the F8.G7 mAb (Figure 6F). Thus, Gal1 blockade limits refractoriness to anti-VEGF treatment.

As previous studies indicate that vascular-targeted strategies should combine mechanisms of vessel pruning with the capacity to promote normalization of the remaining tumor vasculature (Carmeliet and Jain, 2011), we investigated whether Gal1 blockade provided a window of opportunity for tumor vessel normalization. Notably, mAb-mediated Gal1 blockade resulted in substantial remodeling of the vasculature of B16 tumors at days 4–5 posttreatment (Figures 6G–6J). While tumors treated with the isotype control mAb displayed a disorganized and heterogeneous vascular architecture, tumor vasculature from mice treated with F8.G7 mAb resembled normal vascular networks with regard to vessel diameter and distribution (Figure 6G). Moreover, vessels from F8.G7 mAb-treated tumors showed greater coverage by pericytes (Figure 6H), which displayed a more mature phenotype, as revealed by higher expression of α-smooth muscle actin (α-SMA) and lower expression of regulator of G protein signaling 5 (RGS5) and platelet-derived growth factor receptor (PDGFR)-β (Figure 6I). Supporting these findings, administration of F8.G7 mAb markedly alleviated tumor hypoxia as shown by reduced formation of pimonidazole adducts (Figure 6J). However, Gal1 blockade failed to promote vessel normalization later after treatment (data not shown), suggesting the transient nature of this effect. Remarkably, we observed a similar vascular remodeling effect following

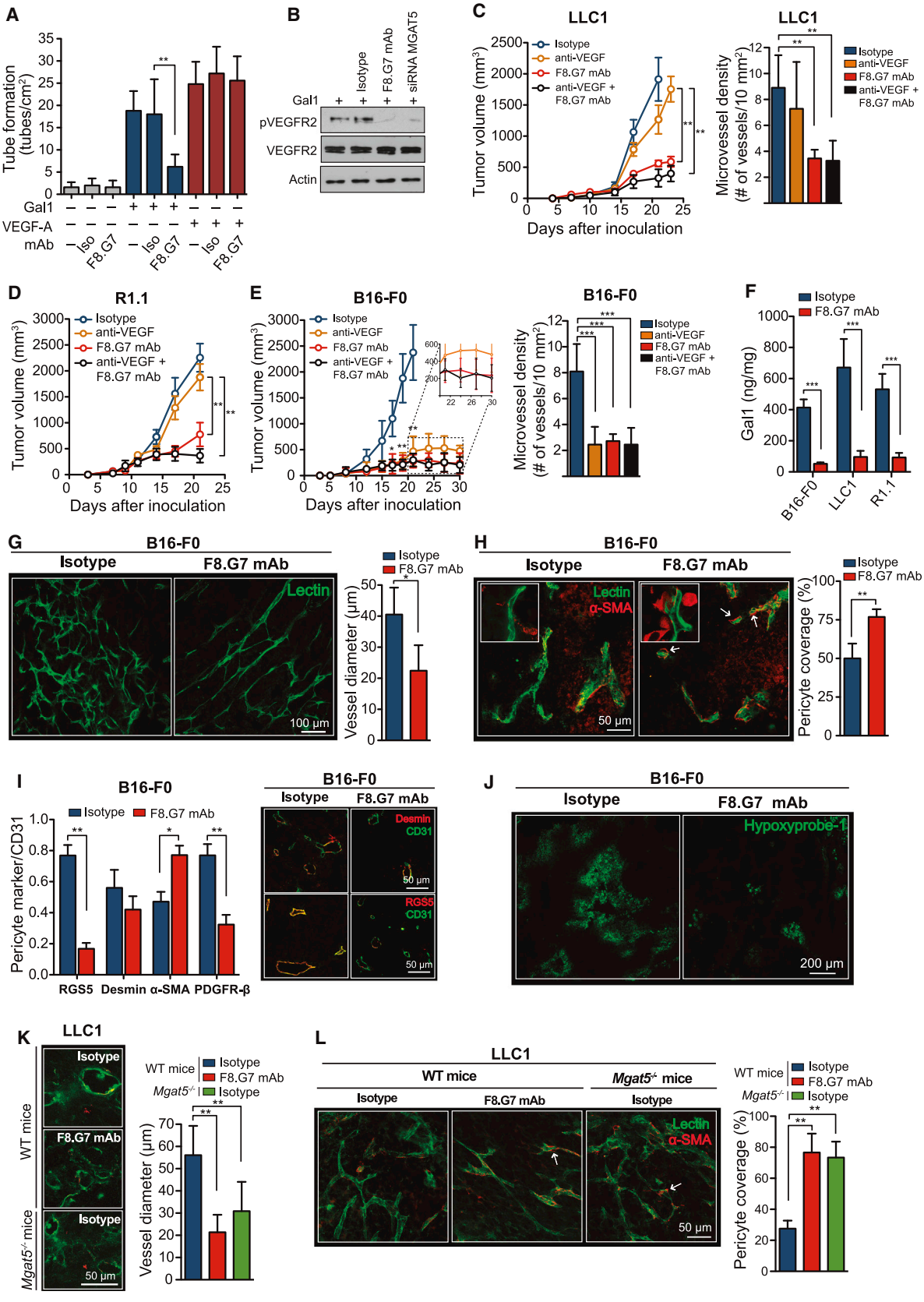

(legend on next page)

administration of F8.G7 mAb into WT mice bearing LLC1 tumors or when tumors were implanted into *Mgat5*$^{-/-}$ mice in the absence of Gal1 blockade (Figures 6K and 6L). Thus, disruption of the Gal1-*N*-glycan axis counteracts the aberrant nature of the tumor vasculature not only by attenuating angiogenesis, but also by modulating vessel morphology early after treatment.

Disruption of Gal1-*N*-Glycan Interactions Affords Therapeutic Benefits through the Control of Both Vascular and Immune Compartments

Because vessel normalization increases the access of immune cells into the tumor (Carmeliet and Jain, 2011) and Gal1 suppresses antitumor immunity (Rubinstein et al., 2004), we sought to dissect the relative contribution of immune and vascular compartments to tumor growth suppression induced by Gal1 blockade. Whereas administration of F8.G7 mAb to tumor-bearing immunocompetent mice resulted in markedly decreased tumor burden (Figures 6C–6E), treatment of immunodeficient *B6.Rag1*$^{-/-}$ mice yielded only a partial antitumor effect (Figure S6A), suggesting the contribution of the immune system to the therapeutic effects of F8.G7 mAb. Accordingly, administration of F8.G7 mAb in mice bearing B16-F0 or LLC1 tumors stimulated T cell proliferation, enhanced IFN-γ and IL-17 secretion, and blunted IL-10 production by tumor-draining lymph node (TDLN) cells (Figures 7A–7G). Moreover, an increase in the number of TDLN and tumor-infiltrating CD8$^+$ T cells was detected in F8.G7 mAb- versus control-treated mice (Figure 7H–7J). To elucidate the contribution of *N*-glycan branching to this effect, we inoculated LLC1 tumors into *Mgat5*$^{-/-}$ mice. Notably, MGAT5 deficiency mirrored the immunostimulatory effects of Gal1 blockade, as revealed by cytokine production and frequency of TDLN and tumor-infiltrating immune cells in tumor-bearing *Mgat5*$^{-/-}$ versus WT mice (Figures 7K–7Q).

To examine whether heightened immunity was, at least in part, mediated by increased access of immune cells due to vessel normalization, T cells obtained from tumor-bearing mice were labeled with CFSE and transferred into mice bearing the same tumor but treated with F8.G7 or isotype control mAb. A greater number of T cells reached the tumor, but not the spleen, in mice receiving F8.G7 mAb as compared to those treated with control isotype (Figure 7R), suggesting increased influx of immune cells subsequent to vessel remodeling. This effect was confirmed using fluorescent beads injected into F8.G7 mAb-treated tumor-bearing WT mice and control-treated tumor-bearing *Mgat5*$^{-/-}$ mice (Figures S6B and S6C), thus validating the contribution of complex *N*-glycans to the vascular remodeling effect. These results emphasize the dual and interrelated effects of blocking Gal1-*N*-glycan interactions, which contribute to restrain tumor growth by attenuating aberrant vascular networks and potentiating tumor immunity.

DISCUSSION

Although underappreciated for many years, recent studies have illuminated the essential contribution of lectin-glycan recognition systems to a variety of biological processes (Rabinovich and Croci, 2012). In this study, we highlight the contribution of the EC glycome to vascular function, integrate the Ga1-*N*-glycan axis into canonical angiogenic pathways, and validate a therapeutic target to surmount anti-VEGF compensatory programs. In addition, our findings underscore the intimate connections between vascular and immune cell programs operating in tumorigenesis.

Multivalent interactions between endogenous lectins and glycans have been shown to function as tuners that, in response to canonical ligands, control cellular responses by adjusting thresholds of cellular signaling (Dennis et al., 2009). However, the high avidity of these interactions (Sacchettini et al., 2001), the remarkable changes displayed by the cellular glycome in physiologic and pathologic settings (Varki et al., 2009) and the pronounced phenotypes observed in mice lacking components of the glycosylation machinery (Ohtsubo and Marth, 2006), suggest that endogenous lectins and glycans might act beyond their tuning function to provide hierarchical "on-and-off" input information that directly activates receptor signaling. Our study shows that direct association of Gal1 with complex *N*-glycans on VEGFR2 Ig3, Ig4, and Ig7 domains may substitute for the absence of VEGF-A to promote EC signaling and preserve the angiogenic phenotype. Although Gal1 could eventually bind other glycosylated receptors, its preferential association with VEGFR2 may reflect differences in α2-6 sialylation, *N*-glycan number and branching and/or protein conformation among individual EC glycoproteins. Tumor-associated stimuli including hypoxia and immunosuppression fuel Gal1 signaling by increasing the availability of nonsialylated complex

Figure 6. Targeting the Gal1-*N*-Glycan Axis Overcomes Anti-VEGF Refractoriness and Promotes Vascular Remodeling

(A) Tube formation of HUVEC treated with Gal1 or VEGF-A with or without anti-Gal1 (F8.G7) or isotype control mAb (mean ± SEM, n = 4; **p < 0.01).

(B) Immunoblot of VEGFR2 phosphorylation in HUVEC treated with Gal1 with or without F8.G7 or isotype control mAb or transfected with MGAT5 siRNA. Representative of three experiments.

(C–E) Growth of LLC1 (C, left), R1.1 (D) and B16-F0 (E, left) and microvessel density (C and E, right) of tumors inoculated in B6 mice and treated with anti-VEGF and/or F8.G7 or isotype control mAb (mean ± SEM, n = 4 with six animals per group; *p < 0.05, **p < 0.01, ***p < 0.001).

(F) ELISA of Gal1 secretion (day 16) by tumors inoculated in B6 mice and treated with F8.G7 or isotype control mAb (mean ± SEM, n = 4 with five animals per group; ***p < 0.001).

(G) Confocal microscopy of lectin (GLS-1_{B4})-perfused vessels in sized-matched B16-F0 tumors inoculated in B6 mice and treated for 4–5 days with F8.G7 or isotype control mAb. Vessel diameter (right).

(H) Confocal microscopy of lectin-perfused vessels (green) and anti-α-SMA Ab (red) in sized-matched B16-F0 tumors inoculated in B6 mice and treated for 4–5 days with F8.G7 or isotype control mAb. Right, percentage of tumor vessels showing pericyte coverage.

(I) Confocal microscopy of RGS5, desmin, α-SMA and PDGFR-β in pericytes associated to vessels of B16-F0 tumors inoculated into B6 mice and treated for 4-5 days with F8.G7 or isotype control mAb. Quantification (left) and representative images (right) are shown.

(J) Confocal microscopy of B16-F0 sized-matched tumors stained with Hypoxiprobe-1. Representative of four experiments.

(K and L) Confocal microscopy of CD31 (K) and lectin-perfused vessels (L, green) and anti-α-SMA Ab (L, red) in LLC1 tumors inoculated into WT mice and treated with F8.G7 or isotype control mAb or inoculated into *Mgat5*$^{-/-}$ mice.

Mean ± SEM, n = 4 with six mice per group (G, H, I, K, and L); *p < 0.05, **p < 0.01. See also Figure S5.

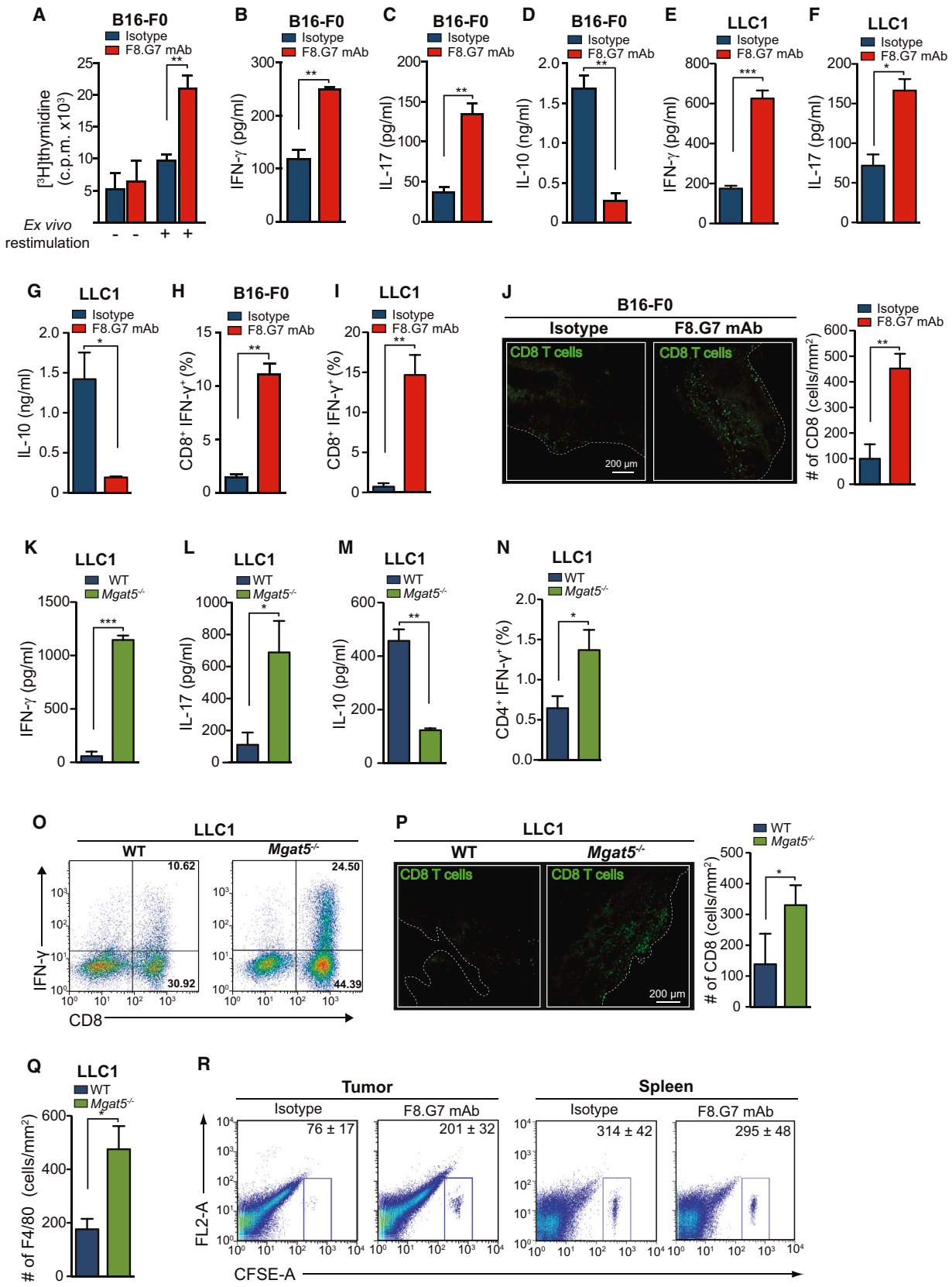

(legend on next page)

N-glycans, whereas proinflammatory signals limit exposure of Gal1 ligands. In this regard, tumor necrosis factor, a major proinflammatory cytokine, can upregulate expression of ST6GAL1 as well as other glycosyltransferases responsible for creating selectin ligands during inflammatory responses (Garcia-Vallejo et al., 2006; Willhauck-Fleckenstein et al., 2010), thus emphasizing the versatility of the EC glycome and its adaptability to cellular physiology. Interestingly, although Gal1-glycan interactions may prolong EC surface residency of VEGFR2 and amplify responses to VEGF-A, our data show that receptor trafficking and signaling may also proceed in the absence of VEGF-A, highlighting the contribution of lectin-glycan recognition to ligand-independent RTK activation. In this regard, previous studies emphasized the relevance of *N*-glycosylation in the signaling capacity of RTKs including epidermal growth factor receptor (EGFR), ErbB2, and ErbB3 (Yokoe et al., 2007; Contessa et al., 2008).

Although approved therapies targeting VEGF have offered significant clinical benefit by improving progression-free and overall survival, some patients experienced decreased benefit over time, suggesting the contribution of compensatory pathways that preserve angiogenesis in VEGF-targeted therapies (Ebos et al., 2009). Although some preclinical reports have yielded conflicting results (Fischer et al., 2007; Bais et al., 2010), vessel pruning induced by VEGF or VEGFR blockade has been shown to aggravate hypoxia, resulting in the upregulation of alternative proangiogenic signals including FGFs, hepatocyte growth factor/c-Met, placental growth factor, Bv8, and IL-17 (Bergers and Hanahan, 2008; Shojaei et al., 2010; Chung et al., 2013). Here, we identified a glycosylation-based circuit, mediated by Gal1-VEGFR2 interactions, that links tumor hypoxia to vascular signaling in anti-VEGF refractory tumors. Remarkably, a "Gal1-permissive" glycophenotype was evident on anti-VEGF refractory, but not sensitive vessels, in response to hypoxia or VEGF blockade. However, hypoxia not only favored the exposure of Gal1-specific ligands, but also promoted Gal1 expression through mechanisms involving NF-κB-activation (Croci et al., 2012). Hence, rather than the upregulation of a single proangiogenic factor, the Gal1-*N*-glycan axis emerges as a synchronized program that is connected with VEGFR2 signaling and bolsters tumor immunosuppressive networks. Although previous studies suggested that VEGFR2 needs to be internalized into early endosomes to signal angiogenesis (Lanahan et al., 2010), recent findings showed that receptor internalization is not required for upstream signaling to proceed, but it is necessary for activating distal kinases (Gourlaouen et al., 2013). We found that Gal1 promoted VEGFR2 internalization with a slower kinetics than VEGF-A, although it triggered full activation of signaling programs.

Although other members of the galectin family, including Gal3 and Gal8, can also promote angiogenesis (Nangia-Makker et al., 2000; Markowska et al., 2011, Delgado et al., 2011), only Gal1 was upregulated in response to VEGF blockade, suggesting that the spatiotemporal regulation of individual galectins, their selective modulation by hypoxia and the repertoire of glycan structures displayed by tumor vessels, together dictate the contribution of individual lectins to angiogenic compensatory programs. In this regard, we found that MGAT5 deficiency increased the efficacy of anti-VEGF treatment, as interruption of β1-6GlcNAc branching prevented Gal1 binding to ECs. Although secreted MGAT5 may also act on heparan sulfate to promote the release of FGF2 through a glycan-independent pathway (Saito et al., 2002), this mechanism is unlikely to operate in our system as FGF2 inhibition did not alter the proangiogenic effect of Gal1, angiogenesis did not occur in the absence of Gal1 and treatment with swainsonine recapitulated the effect of MGAT5 silencing. Moreover, our findings provide an alternative explanation, based on the modulation of vascular and immune compartments, for the reduced tumor growth observed in *Mgat5*$^{-/-}$ mice (Granovsky et al., 2000). Conversely, ST6GAL1 ablation abrogated sensitivity to anti-VEGF treatment, suggesting a major role for α2-6-linked SA in modulating vascularization. This effect was associated with interruption of Gal1-*N*-glycan signaling via VEGFR2, as it was prevented by Gal1 silencing or by administration of axitinib, an RTK inhibitor which preferentially perturbs VEGFRs signaling. Whether activation of the Gal1-*N*-glycan axis contributes to limit the efficacy of VEGF-targeted therapies in human clinical settings remains to be explored.

In this study we document the effects of a neutralizing Gal1-specific mAb that prevented compensatory angiogenesis in anti-VEGF refractory tumors. This therapeutic response did not involve undesired off-target effects, as F8.G7 mAb did not bind to other galectins (Croci et al., 2012), was active at relatively low concentrations (5–10 mg/kg) and phenocopied the consequences of MGAT5 deficiency. Similar to other antiangiogenic agents, mAb-mediated Gal1 blockade not only suppressed tumor vascular supply, but also induced transient vessel normalization as reflected by increased pericyte coverage, alleviation of tumor hypoxia, influx of T cells into the tumor, and subsequent amplification of immune responses. These results underline the dual and interconnected effects of vascular and immune compartments in the context of Gal1 blockade. Importantly, despite the preferential association of Gal1 with VEGFR2, blocking Gal1 would not be equivalent to targeting VEGFR2 as Gal1 could potentially interact with other EC glycosylated receptors and could also modulate tumor growth through

Figure 7. Disruption of Gal1-*N*-Glycan Interactions Controls Both Vascular and Immune Compartments

(A–G) Proliferation (A) and ELISA of IFN-γ (B and E), IL-17 (C and F), and IL-10 (D and G) by TDLN cells from mice inoculated with B16-F0 or LLC1 and treated with F8.G7 or isotype control mAb.

(H and I) Flow cytometry of IFN-γ-producing CD8 T cells in TDLN from mice inoculated with B16-F0 (H) or LLC1 (I) and treated with F8.G7 or isotype control mAb.

(J) Confocal microscopy of tumor-infiltrating CD8 T cells in mice inoculated with B16-F0 and treated with F8.G7 or isotype control mAb.

(K–O) ELISA of IFN-γ (K), IL-17 (L), and IL-10 (M), and flow cytometry (N and O) of IFN-γ-producing CD4 (N) or CD8 (O) T cells in TDLN from *Mgat5*$^{-/-}$ or WT mice inoculated with LLC1.

(P and Q) Confocal microscopy of tumor-infiltrating CD8 T cells (P) and F4/80^{+} macrophages (Q) in *Mgat5*$^{-/-}$ or WT mice inoculated with LLC1.

(R) Flow cytometry of CFSE^{+} transferred T cells reaching the tumor or spleen.

Data are the mean ± SEM (A-N, P,Q) or are representative (J left, O, P left, R) of n = 4 experiments with six mice per group. *$p < 0.05$, **$p < 0.01$, ***$p < 0.001$. See also Figure S6.

vascular-independent immune-related mechanisms (Banh et al., 2011). In this regard, resistance to RTK inhibitors has also been described in preclinical models (Shojaei et al., 2010), posing the challenge of tailoring targeted therapies based on the identification of individual compensatory programs. Finally, given its immunostimulatory effects, targeting the Gal1-*N*-glycan axis may also complement immunotherapeutic modalities aimed at releasing the brakes of tumor immunity, including those involving CTLA-4 or PD-1/PD-L1 blockade (Coussens et al., 2013).

In conclusion, we identified a glycosylation-based circuit that links tumor hypoxia, VEGFR2 signaling and compensatory angiogenesis in the context of VEGF blockade. These findings may have broader implications in other clinical settings involving dysregulated angiogenesis including age-related macular degeneration, diabetes retinopathy, and cardiovascular diseases.

EXPERIMENTAL PROCEDURES

Mice

Lgals1$^{-/-}$ mice were provided by F. Poirier, *Mgat5*$^{-/-}$ mice were provided by J. Dennis and *St6gal1*$^{-/-}$ mice were provided by J. Paulson. Mice were bred at the animal facility of IBYME according to NIH guidelines. Protocols were approved by the institutional review board.

Glycophenotyping

Cells were incubated with biotinylated lectins (Vector) or 488-labeled Gal1 as described (Toscano et al., 2007).

Angiogenesis Assays

ECs transfected with MGAT5, C2GNT1 or scr siRNA were exposed to VEGF-A or Gal1 with or without lactose, anti-VEGFR1 (AP-MAB0702), anti-VEGFR3 (AB89501), mAb (from Abcam) or anti-VEGF-A (MAB293), anti-VEGFR2 (AF357), anti-$\alpha_V\beta_3$ (MAB3050), anti-α_5 (AF1864), anti-β_1 (MAB17781) integrin mAb or isotype control IgG1κ (all from R&D) or anti-Gal1 (F8.G7) mAb. Cells were processed for proliferation, migration, and tube formation as described (Croci et al., 2012). Tumor-associated ECs were identified by flow cytometry using 647-conjugated anti-CD34 (RAM34; eBioscience) and FITC-conjugated anti-CD45 (J33; Immunotech). Microvessel density reflected the number of CD31$^+$ microvessels present in 10 mm^2.

Tumor Models

Wild-type or Gal1 knockdown B16-F0, LLC1, and R1.1 (2.5 or 5 × 10^5 cells) were s.c. inoculated into 6- to 8-week old WT, *Mgat5*$^{-/-}$, *St6gal1*$^{-/-}$, *Lgals1*$^{-/-}$, or *Rag1*$^{-/-}$ B6 mice. CT26 (5 × 10^5) cells were injected into BALB/c mice. When tumors reached 100 mm^3, mice were inoculated i.p. with anti-VEGF (B20-4.1.1; 5 or 10 mg/kg) and/or anti-Gal1 (F8.G7; 5, 10 or 15 mg/kg) mAb or control mAb twice weekly. Axitinib (30 mg/kg; Sigma) was administered every 2 days by oral gavage. Mice were sacrificed when tumors reached a volume greater than 2.5 cm^3. Two weeks after tumor inoculation, TDLN cells (5 × 10^5/ well) were restimulated ex vivo for 72 hr with tumor lysates and analyzed for proliferation and cytokine production as described (Rubinstein et al., 2004).

Statistical Analysis

Prism software (GraphPad) was used for statistical analysis. Student's t test was used for unpaired data. Two-way ANOVA and Dunnett's or Tukey post-tests were used for multiple comparisons. p values of 0.05 or less were considered significant.

SUPPLEMENTAL INFORMATION

Supplemental Information includes Extended Experimental Procedures and six figures and can be found with this article online at http://dx.doi.org/10.1016/j.cell.2014.01.043.

ACKNOWLEDGMENTS

We thank J. Dennis for *Mgat5*$^{-/-}$ mice; J. Paulson for *St6gal1*$^{-/-}$ mice; F. Poirier for *Lgals1*$^{-/-}$ mice; J. Wang for Gal1^{N46D}; C. Tran for PDAC tumors; J. Stupirski, H. Kalay, C. Leishman, and R. Morales for technical assistance; and J. Ilarregui and A. Góngora for advice. Supported by the Argentinean Agency for Promotion of Science and Technology, CONICET, University of Buenos Aires, Sales Foundation, and donations from Ferioli and Ostry families (to G.A.R.).

Received: July 19, 2013
Revised: November 11, 2013
Accepted: January 21, 2014
Published: February 13, 2014

REFERENCES

Bais, C., Wu, X., Yao, J., Yang, S., Crawford, Y., McCutcheon, K., Tan, C., Kolumam, G., Vernes, J.M., Eastham-Anderson, J., et al. (2010). PlGF blockade does not inhibit angiogenesis during primary tumor growth. Cell *141*, 166–177.

Banh, A., Zhang, J., Cao, H., Bouley, D.M., Kwok, S., Kong, C., Giaccia, A.J., Koong, A.C., and Le, Q.T. (2011). Tumor galectin-1 mediates tumor growth and metastasis through regulation of T-cell apoptosis. Cancer Res. *71*, 4423–4431.

Benedito, R., Roca, C., Sörensen, I., Adams, S., Gossler, A., Fruttiger, M., and Adams, R.H. (2009). The notch ligands Dll4 and Jagged1 have opposing effects on angiogenesis. Cell *137*, 1124–1135.

Bergers, G., and Hanahan, D. (2008). Modes of resistance to anti-angiogenic therapy. Nat. Rev. Cancer *8*, 592–603.

Carmeliet, P., and Jain, R.K. (2011). Molecular mechanisms and clinical applications of angiogenesis. Nature *473*, 298–307.

Chung, A.S., and Ferrara, N. (2011). Developmental and pathological angiogenesis. Annu. Rev. Cell Dev. Biol. *27*, 563–584.

Chung, A.S., Wu, X., Zhuang, G., Ngu, H., Kasman, I., Zhang, J., Vernes, J.M., Jiang, Z., Meng, Y.G., Peale, F.V., et al. (2013). An interleukin-17-mediated paracrine network promotes tumor resistance to anti-angiogenic therapy. Nat. Med. *19*, 1114–1123.

Contessa, J.N., Bhojani, M.S., Freeze, H.H., Rehemtulla, A., and Lawrence, T.S. (2008). Inhibition of N-linked glycosylation disrupts receptor tyrosine kinase signaling in tumor cells. Cancer Res. *68*, 3803–3809.

Coussens, L.M., Zitvogel, L., and Palucka, A.K. (2013). Neutralizing tumor-promoting chronic inflammation: a magic bullet? Science *339*, 286–291.

Croci, D.O., Salatino, M., Rubinstein, N., Cerliani, J.P., Cavallin, L.E., Leung, H.J., Ouyang, J., Ilarregui, J.M., Toscano, M.A., Domaica, C.I., et al. (2012). Disrupting galectin-1 interactions with N-glycans suppresses hypoxia-driven angiogenesis and tumorigenesis in Kaposi's sarcoma. J. Exp. Med. *209*, 1985–2000.

D'Haene, N., Sauvage, S., Maris, C., Adanja, I., Le Mercier, M., Decaestecker, C., Baum, L., and Salmon, I. (2013). VEGFR1 and VEGFR2 involvement in extracellular galectin-1- and galectin-3-induced angiogenesis. PLoS ONE *8*, e67029.

Dalotto-Moreno, T., Croci, D.O., Cerliani, J.P., Martinez-Allo, V.C., Dergan-Dylon, S., Méndez-Huergo, S.P., Stupirski, J.C., Mazal, D., Osinaga, E., Toscano, M.A., et al. (2013). Targeting galectin-1 overcomes breast cancer-associated immunosuppression and prevents metastatic disease. Cancer Res. *73*, 1107–1117.

Delgado, V.M., Nugnes, L.G., Colombo, L.L., Troncoso, M.F., Fernández, M.M., Malchiodi, E.L., Frahm, I., Croci, D.O., Compagno, D., Rabinovich, G.A., et al. (2011). Modulation of endothelial cell migration and angiogenesis: a novel function for the "tandem-repeat" lectin galectin-8. FASEB J. *25*, 242–254.

Dennis, J.W., Nabi, I.R., and Demetriou, M. (2009). Metabolism, cell surface organization, and disease. Cell *139*, 1229–1241.

Ebos, J.M., Lee, C.R., and Kerbel, R.S. (2009). Tumor and host-mediated pathways of resistance and disease progression in response to antiangiogenic therapy. Clin. Cancer Res. *15*, 5020–5025.

Ellis, L.M., and Hicklin, D.J. (2008). VEGF-targeted therapy: mechanisms of anti-tumour activity. Nat. Rev. Cancer *8*, 579–591.

Fischer, C., Jonckx, B., Mazzone, M., Zacchigna, S., Loges, S., Pattarini, L., Chorianopoulos, E., Liesenborghs, L., Koch, M., De Mol, M., et al. (2007). Anti-PlGF inhibits growth of VEGF(R)-inhibitor-resistant tumors without affecting healthy vessels. Cell *131*, 463–475.

Fu, J., Gerhardt, H., McDaniel, J.M., Xia, B., Liu, X., Ivanciu, L., Ny, A., Hermans, K., Silasi-Mansat, R., McGee, S., et al. (2008). Endothelial cell O-glycan deficiency causes blood/lymphatic misconnections and consequent fatty liver disease in mice. J. Clin. Invest. *118*, 3725–3737.

Garcia-Vallejo, J.J., Van Dijk, W., Van Het Hof, B., Van Die, I., Engelse, M.A., Van Hinsbergh, V.W., and Gringhuis, S.I. (2006). Activation of human endothelial cells by tumor necrosis factor-alpha results in profound changes in the expression of glycosylation-related genes. J. Cell. Physiol. *206*, 203–210.

Gourlaouen, M., Welti, J.C., Vasudev, N.S., and Reynolds, A.R. (2013). Essential role for endocytosis in the growth factor-stimulated activation of ERK1/2 in endothelial cells. J. Biol. Chem. *288*, 7467–7480.

Granovsky, M., Fata, J., Pawling, J., Muller, W.J., Khokha, R., and Dennis, J.W. (2000). Suppression of tumor growth and metastasis in Mgat5-deficient mice. Nat. Med. *6*, 306–312.

Hart, G.W., and Copeland, R.J. (2010). Glycomics hits the big time. Cell *143*, 672–676.

Hsieh, S.H., Ying, N.W., Wu, M.H., Chiang, W.F., Hsu, C.L., Wong, T.Y., Jin, Y.T., Hong, T.M., and Chen, Y.L. (2008). Galectin-1, a novel ligand of neuropilin-1, activates VEGFR-2 signaling and modulates the migration of vascular endothelial cells. Oncogene *27*, 3746–3753.

Kitazume, S., Imamaki, R., Ogawa, K., Komi, Y., Futakawa, S., Kojima, S., Hashimoto, Y., Marth, J.D., Paulson, J.C., and Taniguchi, N. (2010). Alpha2,6-sialic acid on platelet endothelial cell adhesion molecule (PECAM) regulates its homophilic interactions and downstream antiapoptotic signaling. J. Biol. Chem. *285*, 6515–6521.

Laderach, D.J., Gentilini, L.D., Giribaldi, L., Delgado, V.C., Nugnes, L., Croci, D.O., Al Nakouzi, N., Sacca, P., Casas, G., Mazza, O., et al. (2013). A unique galectin signature in human prostate cancer progression suggests galectin-1 as a key target for treatment of advanced disease. Cancer Res. *73*, 86–96.

Lanahan, A.A., Hermans, K., Claes, F., Kerley-Hamilton, J.S., Zhuang, Z.W., Giordano, F.J., Carmeliet, P., and Simons, M. (2010). VEGF receptor 2 endocytic trafficking regulates arterial morphogenesis. Dev. Cell *18*, 713–724.

Le, Q.T., Shi, G., Cao, H., Nelson, D.W., Wang, Y., Chen, E.Y., Zhao, S., Kong, C., Richardson, D., O'Byrne, K.J., et al. (2005). Galectin-1: a link between tumor hypoxia and tumor immune privilege. J. Clin. Oncol. *23*, 8932–8941.

Lee, S., Chen, T.T., Barber, C.L., Jordan, M.C., Murdock, J., Desai, S., Ferrara, N., Nagy, A., Roos, K.P., and Iruela-Arispe, M.L. (2007). Autocrine VEGF signaling is required for vascular homeostasis. Cell *130*, 691–703.

López-Lucendo, M.F., Solís, D., André, S., Hirabayashi, J., Kasai, K., Kaltner, H., Gabius, H.J., and Romero, A. (2004). Growth-regulatory human galectin-1: crystallographic characterisation of the structural changes induced by single-site mutations and their impact on the thermodynamics of ligand binding. J. Mol. Biol. *343*, 957–970.

Markowska, A.I., Jefferies, K.C., and Panjwani, N. (2011). Galectin-3 protein modulates cell surface expression and activation of vascular endothelial growth factor receptor 2 in human endothelial cells. J. Biol. Chem. *286*, 29913–29921.

Mathieu, V., de Lassalle, E.M., Toelen, J., Mohr, T., Bellahcène, A., Van Goietsenoven, G., Verschuere, T., Bouzin, C., Debyser, Z., De Vleeschouwer, S., et al. (2012). Galectin-1 in melanoma biology and related neo-angiogenesis processes. J. Invest. Dermatol. *132*, 2245–2254.

Nangia-Makker, P., Honjo, Y., Sarvis, R., Akahani, S., Hogan, V., Pienta, K.J., and Raz, A. (2000). Galectin-3 induces endothelial cell morphogenesis and angiogenesis. Am. J. Pathol. *156*, 899–909.

Ohtsubo, K., and Marth, J.D. (2006). Glycosylation in cellular mechanisms of health and disease. Cell *126*, 855–867.

Olsson, A.K., Dimberg, A., Kreuger, J., and Claesson-Welsh, L. (2006). VEGF receptor signalling - in control of vascular function. Nat. Rev. Mol. Cell Biol. *7*, 359–371.

Potente, M., Gerhardt, H., and Carmeliet, P. (2011). Basic and therapeutic aspects of angiogenesis. Cell *146*, 873–887.

Rabinovich, G.A., and Croci, D.O. (2012). Regulatory circuits mediated by lectin-glycan interactions in autoimmunity and cancer. Immunity *36*, 322–335.

Rubinstein, N., Alvarez, M., Zwirner, N.W., Toscano, M.A., Ilarregui, J.M., Bravo, A., Mordoh, J., Fainboim, L., Podhajcer, O.L., and Rabinovich, G.A. (2004). Targeted inhibition of galectin-1 gene expression in tumor cells results in heightened T cell-mediated rejection; A potential mechanism of tumor-immune privilege. Cancer Cell *5*, 241–251.

Sacchettini, J.C., Baum, L.G., and Brewer, C.F. (2001). Multivalent protein-carbohydrate interactions. A new paradigm for supermolecular assembly and signal transduction. Biochemistry *40*, 3009–3015.

Saito, T., Miyoshi, E., Sasai, K., Nakano, N., Eguchi, H., Honke, K., and Taniguchi, N. (2002). A secreted type of β 1,6-N-acetylglucosaminyltransferase V (GnT-V) induces tumor angiogenesis without mediation of glycosylation: a novel function of GnT-V distinct from the original glycosyltransferase activity. J. Biol. Chem. *277*, 17002–17008.

Shojaei, F., Wu, X., Malik, A.K., Zhong, C., Baldwin, M.E., Schanz, S., Fuh, G., Gerber, H.P., and Ferrara, N. (2007). Tumor refractoriness to anti-VEGF treatment is mediated by CD11b+Gr1+ myeloid cells. Nat. Biotechnol. *25*, 911–920.

Shojaei, F., Lee, J.H., Simmons, B.H., Wong, A., Esparza, C.O., Plumlee, P.A., Feng, J., Stewart, A.E., Hu-Lowe, D.D., and Christensen, J.G. (2010). HGF/c-Met acts as an alternative angiogenic pathway in sunitinib-resistant tumors. Cancer Res. *70*, 10090–10100.

Singh, M., Lima, A., Molina, R., Hamilton, P., Clermont, A.C., Devasthali, V., Thompson, J.D., Cheng, J.H., Bou Reslan, H., Ho, C.C.K., et al. (2010). Assessing therapeutic responses in *Kras* mutant cancers using genetically engineered mouse models. Nat. Biotechnol. *28*, 585–593.

Song, Y., Aglipay, J.A., Bernstein, J.D., Goswami, S., and Stanley, P. (2010). The bisecting GlcNAc on N-glycans inhibits growth factor signaling and retards mammary tumor progression. Cancer Res. *70*, 3361–3371.

Thijssen, V.L., Postel, R., Brandwijk, R.J., Dings, R.P., Nesmelova, I., Satijn, S., Verhofstad, N., Nakabeppu, Y., Baum, L.G., Bakkers, J., et al. (2006). Galectin-1 is essential in tumor angiogenesis and is a target for antiangiogenesis therapy. Proc. Natl. Acad. Sci. USA *103*, 15975–15980.

Thijssen, V.L., Barkan, B., Shoji, H., Aries, I.M., Mathieu, V., Deltour, L., Hackeng, T.M., Kiss, R., Kloog, Y., Poirier, F., and Griffioen, A.W. (2010). Tumor cells secrete galectin-1 to enhance endothelial cell activity. Cancer Res. *70*, 6216–6224.

Toscano, M.A., Bianco, G.A., Ilarregui, J.M., Croci, D.O., Correale, J., Hernandez, J.D., Zwirner, N.W., Poirier, F., Riley, E.M., Baum, L.G., and Rabinovich, G.A. (2007). Differential glycosylation of T_H1, T_H2 and T_H17 effector cells selectively regulates susceptibility to cell death. Nat. Immunol. *8*, 825–834.

Varki, A., Kannagi, R., and Toole, B.P. (2009). Glycosylation changes in cancer. In Essentials of Glycobiology, Second Edition, A. Varki, R.D. Cummings, J.D. Esko, H.H. Freeze, P. Stanley, C.R. Bertozzi, G.W. Hart, and M.E. Etzler, eds. (Cold Spring Harbor, NY: Cold Spring Harbor Laboratory Press).

Willhauck-Fleckenstein, M., Moehler, T.M., Merling, A., Pusunc, S., Goldschmidt, H., and Schwartz-Albiez, R. (2010). Transcriptional regulation of the vascular endothelial glycome by angiogenic and inflammatory signalling. Angiogenesis *13*, 25–42.

Xu, D., Fuster, M.M., Lawrence, R., and Esko, J.D. (2011). Heparan sulfate regulates VEGF165- and VEGF121-mediated vascular hyperpermeability. J. Biol. Chem. *286*, 737–745.

Yokoe, S., Takahashi, M., Asahi, M., Lee, S.H., Li, W., Osumi, D., Miyoshi, E., and Taniguchi, N. (2007). The Asn418-linked N-glycan of ErbB3 plays a crucial role in preventing spontaneous heterodimerization and tumor promotion. Cancer Res. *67*, 1935–1942.